



All Solid-State Lithium-Polymer Battery Using a Self-Cross-Linking Polymer Electrolyte

Congxiao Wang,^a Tetsuo Sakai,^{a,*} Osamu Watanabe,^b Kazuhiro Hirahara,^b and Toru Nakanishi^b

^aNational Institute of Advanced Industrial Science and Technology (AIST), Kansai Collaboration Center, Ikeda, Osaka 563-8577, Japan

^bShin-Etsu Chemical Company, Limited, Kashima-gun, Ibaraki, Japan

A self-cross-linking polymer electrolyte based on polystyrene-incorporated poly(ethylene oxide) (PEO) containing LiTFSI has been tested in an all solid-state lithium-polymer battery (Li/SP-E/Li_xMnO₂ with a solid polymer electrolyte. The polymer electrolyte showed high stability toward metallic lithium. Mechanical properties of the electrolyte film were much improved by incorporating the polystyrene, but ion conductivity was decreased to half of the value obtained in pure PEO electrolyte film. The cell was charged and discharged at a high temperature (80°C), providing about 80% utilization of the positive electrode. The cell showed good cycle life at 80°C, keeping 90% of the initial capacity after 50 cycles.

© 2003 The Electrochemical Society. [DOI: 10.1149/1.1593652] All rights reserved.

Manuscript submitted September 3, 2002; revised manuscript received January 22, 2003. Available electronically July 10, 2003.

Lithium-ion technology is rapidly contributing to the state-of-art of secondary systems and has been commercially used in popular portable devices such as cellular phones and note-size computers. However, such batteries are not being rapidly developed for electric vehicles (EVs) in view of the safety of the devices because the use of a liquid electrolyte may result in problems, *i.e.*, leakage of a flammable electrolyte, production of gases upon overcharge or over-discharge, and a thermal runaway reaction when the battery is heated to high temperatures. On the other hand, an all solid-state lithium/polymer battery (LPB) using a metallic lithium anode and solvent-free polymer electrolyte has been demonstrated to be the most promising secondary battery for EV applications because of its absence of risk for leakage of liquid electrolyte, its higher energy density, and its shape flexibility. One of the paramount approaches is to use a thin film of polymer electrolyte with high ionic conductivity and strong mechanical integrity.¹⁻⁹ High ionic conductivity is expected to improve rate capability. Good mechanical properties are required to protect against shortages, to assure safety reliability, and to make a feasible thin film, thus improving battery-specific energy and rate capability. However, it is difficult to optimize both the energy and rate capability. In the present work, we used a polystyrene-poly(ethylene oxide) (PEO) block-graft copolymer, which has a microphase-separated structure, a lamellar shape, good ionic conductivity, and excellent mechanical properties, as the polymer electrolyte for a Li/Li_xMnO₂ cell. The electrochemical performance, especially the effect of the film thickness on rate capability, was evaluated.

Experimental

The detailed synthesis condition of the polystyrene-poly(ethylene oxide) block-graft copolymer (SE-P) is reported elsewhere.¹⁰ The structure of the polymer is shown in Fig. 1. The average molecular weight is 3.4×10^5 with an ethylene oxide (EO) content of 60 wt %. Battery-grade lithium bis(trifluoromethanesulfonyl)imide (LiTFSI Kishida Chemical Co., Ltd) was used as the electrolyte salt and was vacuum dried for 24 h before use. The polymer electrolyte film was prepared by a well-known solvent-casting technique: a known amount of SE-P and LiTFSI, normally an EO/Li ratio of 20/1, was dissolved in tetrahydrofuran solvent and stirred continuously for 24 h to form a homogenous mixture. The mixture was cast onto a Mylar sheet. The solvent was allowed to evaporate at room temperature for 24 h and the samples were then vacuum dried at room temperature to give an electrolyte film with an average thickness of 30 to 100 μm . The electrolyte films were further vacuum

dried at 80°C for 24 h before use. The fabrication of polymer membranes was carried in a dry room with the dew point less than -60° .

The dynamic Young's modulus data were measured by using a RSA2 (Rheometric Scientific F.E. Ltd.). The heating rate was 5°C/min, and the frequency was 1 Hz. The conductivity of the polymer electrolyte film was measured using ac impedance by placing the sample into a two block electrode (stainless steel, SS) cell. The electrode area was 1 cm², and the thickness 50 μm . The ac impedance experiments were carried out using an EG&G PAR potentiostat coupled with a model 1250 frequency response analyzer controlled by a computer. The temperature ranged from 30 to 100°C. The impedance spectra were normally recorded from 100 kHz to 0.1 Hz and the ac oscillation amplitude was 5 mV. The stability of the polymer electrolyte/lithium metal electrode interface was also evaluated by monitoring the cycle dependence of the impedance response of a symmetrical Li/SPE/Li cell. The ac impedance measurements were fitted into an equivalent circuit by using ZSimp Win software.

The thermal stability of the polymer electrolyte itself and of the polymer electrolyte in contact with metallic lithium was characterized by differential scanning calorimetry (DSC). Experiments were conducted using a thermal analyzer system (DSC8230, Rigaku Ltd., Japan) at a heating rate of 10°C/min with a 50 mL/min Ar flow rate. About 5 mg of the sample was well sealed in an aluminum DSC pan.

The cathode material, Li_{0.33}MnO₂, was prepared by preheating a mixture of LiNO₃ and MnO₂ at 260°C for 5 h, followed by heating at 320°C for 12 h in air.^{11,12} The preparation process of the composite cathode was as follows: a mixture of 65 wt % active material, 5 wt % carbon (Ketjen black), and 30 wt % P(EO)₂₀LiN(CF₃SO₂)₂ (here using P(EO) Mw = 2000) was well mixed and pressed on an Al mesh using hot-pressing techniques. The thickness of the composite positive electrode examined here (excluding the thickness of Al foil) was about 30 μm , and the active mass loading was about 3 mg.

The Li/polymer-electrolyte/Li_{0.33}MnO₂ cell performance was characterized in CR2032 coin-type hardware. Cells were cycled between 2.0 and 3.5 V at 80°C. The typical current rate was C/6 (0.1 mA/cm², 20 mA/g), except where otherwise specified.

Results and Discussion

Polystyrene-PEO block-graft copolymer.—As shown in Fig. 1, the block-graft copolymer showed a microphase-separated structure (MS) consisting of a backbone molecule of polystyrene and a graft molecule of PEO. The MS structure can be clearly seen in the transmission electron micrograph (TEM) shown in Fig. 2. The black and white regions correspond to the PEO phases and polystyrene phase, respectively. The detailed discussion about the structure and proper-

* Electrochemical Society Active Member.

^z E-mail: sakai-tetsuo@aist.go.jp

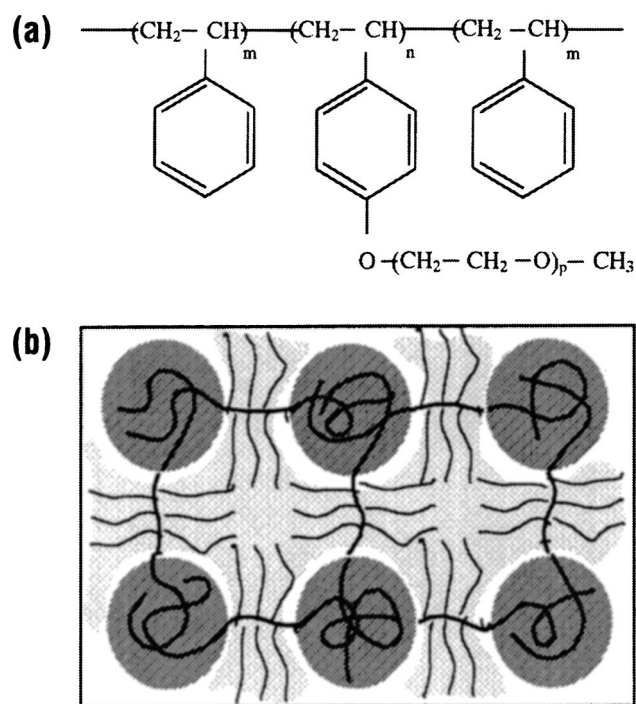


Figure 1. (a) Structure of block-graft copolymer film and (b) schematic presentation of its structure.

ties for the MS polymer could be found in the previous work of one of the authors.¹⁰ The dynamics modulus data are given in Fig. 3. The polystyrene showed good mechanical strength but broken at 65°C. The introduction of an EO elastic component compensated for the fragility of the styrene component up to 100°C. Figure 4 shows the temperature dependence of conductivity of the block-graft copolymer electrolyte compared with PEO during the first heating. The Arrhenius plot shows that the ionic conductivity of the block-graft copolymer electrolyte was a little lower than that of the PEO, but reasonable values, *e.g.*, $\sigma > 10^{-4} \text{ S cm}^{-1}$ at 60°C, were achieved. The major difference was observed below 60°C. The block-graft copolymer clearly showed conductivity enhancements below 60°C. The crystalline-amorphous transition (60°C) of PEO was not observed, even though the block-graft copolymer contained PEO seg-

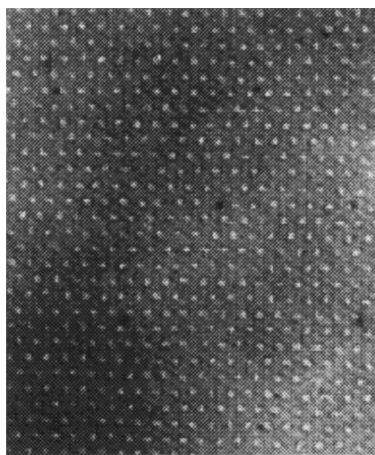


Figure 2. Transmission electron micrograph of block-graft copolymer film (EO: 60 wt %). (Black region corresponds to PEO phase and white region to polystyrene phase.

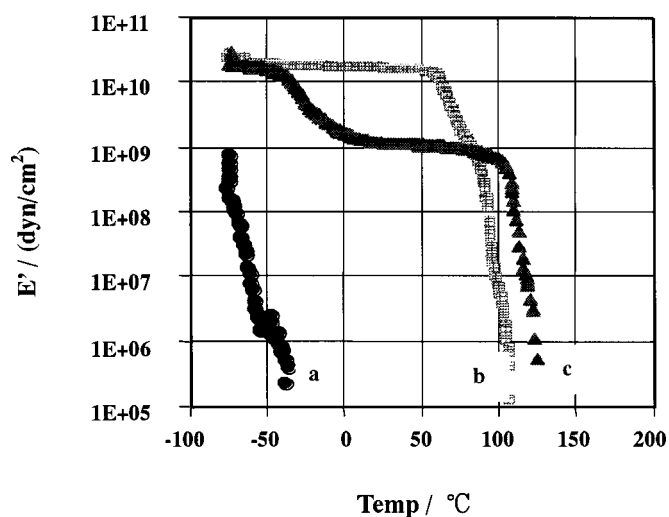


Figure 3. Dynamics moduli data of block-graft copolymer film: (a) PEO, (b) polystyrene, and (c) SE-P + LiTFSI.

ments. A detailed explanation of why the PEO segments in the block-graft copolymer became not crystalline but amorphous can be found in the literature.¹³⁻¹⁵

Interfacial stability with metallic lithium and cathode.—The electrochemical stability of the block-graft copolymer on a smooth blocking electrode (a platinum working electrode) was reported to be stable up to 4.5 V vs. Li/Li⁺ at 80°C in Ref. 10. However, as demonstrated in our previous work,¹⁶ in a real battery system, a polymer electrolyte works with a composite electrode rather than a smooth inert electrode. In the composite cathode, the polymer electrolyte is in contact with the active material and conductive material, *e.g.*, carbon black, acetylene black, graphite, etc. Figure 5 shows the linear sweep voltammogram Li/SE-P/carbon composite at a scan rate of 1 mV/s. The figure clearly shows that the decomposition of the block-graft copolymer started at 3.8 V vs. Li/Li⁺ on a carbon composite electrode, about 1 V below the value obtained with a smooth, inert electrode, indicating that the block-graft copolymer may show high potential for battery application in combination with 3 V cathode materials.

The interfacial stability between the lithium electrode and the polymer electrolyte was evaluated by monitoring the cycle dependence of both the overvoltage and the impedance response of a

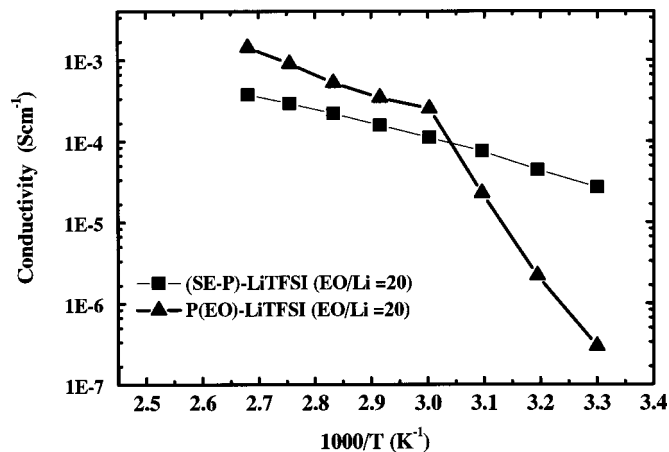


Figure 4. The temperature dependence of the conductivity of a block-graft copolymer electrolyte compared with a similar PEO electrolyte during first heating.

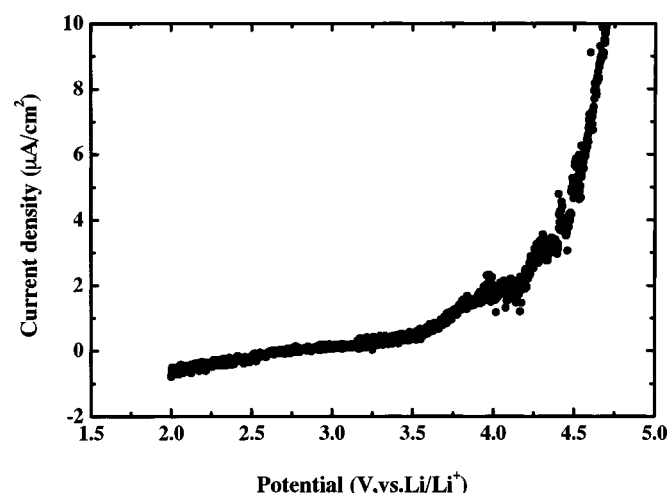


Figure 5. The linear sweep voltammogram of Li/SE-P/carbon composite cell at a scan rate of 1 mV/s at 80°C.

symmetric Li/solid polymer electrolyte/Li cell during the plating/stripping cycle. Cells were cycled at 0.1 mA/cm² for 1 h at 80°C. The value of the voltage at the end of each plating/stripping cycle is directly linked to the overall cell impedance, which is very sensitive to the variations in the passive layer on the lithium electrodes. As shown in Fig. 6, the cells containing the block-graft copolymer electrolyte showed a very constant voltage of 20 mV over 200 cycles, indicative of high stability with metallic lithium. The ac impedance spectra at different cycles are given in Fig. 7. The ac spectra at all cycles showed a slightly depressed semicircle associated with the Li/polymer electrolyte interfacial process. A 45° line followed the semicircle, typical of Warburg impedance due to lithium-ion diffusion phenomena. Hardly any impedance shift at a high frequency was detected, suggesting that there was no electrolyte thickness change upon cycling at 80°C because of the good mechanical properties of the block-graft copolymer electrolyte. The ac impedance measurements were fitted into an equivalent circuit by using Zsimp Win software according to the simple model proposed by Appetechi,¹⁷ as shown in Fig. 8, in which the contribution of the Li/polymer electrolyte interfacial impedance was simply used as the interfacial resistance $R_{(PE/Li)}$ parameter and a constant-phase element (CPE) parameter ($Q_{(PE/Li)}$ and n) related to interfacial capacitance. The fitted results of the experimental spectra after various

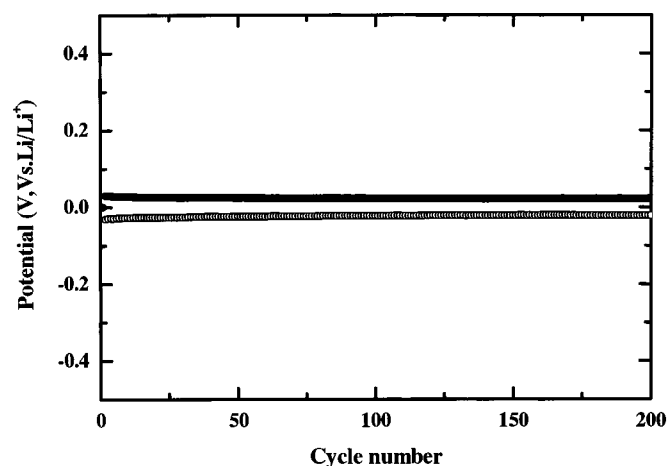


Figure 6. Stability of block-graft copolymer film toward lithium using a symmetric Li/SE-P/Li cell during plating/stripping cycles. Cell was cycled at 0.1 mA/cm² for 1 h at 80°C.

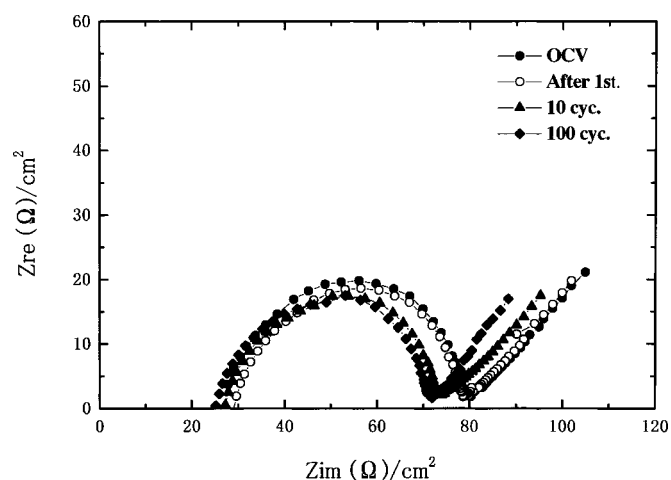
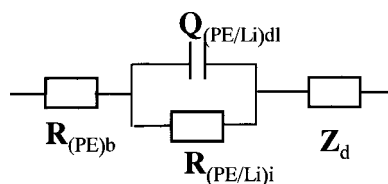


Figure 7. The ac impedance spectra of a Li/SE-P/Li cell at different cycles at 80°C.

cycles are summarized in Table I. The results show that Li/polymer electrolyte interface resistance increased only about 5 Ω after 200 cycles, indicative of a highly stable interfacial between the metallic lithium and the block-graft copolymer.

The thermal stability of the polymer electrolyte itself and in contact with metallic lithium was also characterized. Figure 9 gives the DSC traces of a block-graft copolymer and the polymer in contact with metallic lithium from 25 to 300°C. The block-graft copolymer was at least thermally stable up to 300°C. When the block-graft copolymer was in contact with metallic lithium, one pair of reversible endothermic and exothermic peaks at 180°C was solely detected, which could be attributed to the melting/solidifying of metallic lithium, indicating that the block-graft copolymer is thermally stable with metallic lithium over a temperature range of 25 and 300°C.

Li/SPE/Li_xMnO₂.—As demonstrated above, the block-graft copolymer electrolyte is stable up to 3.8 V vs. Li/Li⁺ against a carbon-containing electrode. We selected 3 V Li_xMnO₂ as a cathode to assemble a Li/solid polymer electrolyte/Li_xMnO₂ cell. The crystal structure of Li_xMnO₂ is similar to that of γ-MnO₂, indexed to ordered alternating one-dimensional (1 × 2) and (1 × 1) channels.¹⁸ Li_xMnO₂ has a theoretical capacity of 207 mAh/g, corresponding to 0.67 mol Li⁺ intercalation into the Li_xMnO₂ framework. The detailed synthesis condition and the electrochemical behavior in the liquid electrolyte can be found elsewhere.¹¹ Figure 10 shows the discharge curves of Li/Li_xMnO₂ containing a 50 μm thick SE-P polymer electrolyte film at temperatures varying from 40 to 80°C. The cell could be operated at 40°C, and it delivered a capacity of 110 mAh/g at 0.125 mA/cm², corresponding to 65% of the initial utilization of Li_xMnO₂. It was almost independent at an operating



$R_{(PE)b}$ = bulk resistance; Z_d = diffusive impedance

$Q_{(PE/Li)dl}$ = double layer capacitance; $R_{(PE/Li)i}$ = interface resistance

Figure 8. The equivalent circuit for Li/SE-P/Li cell.

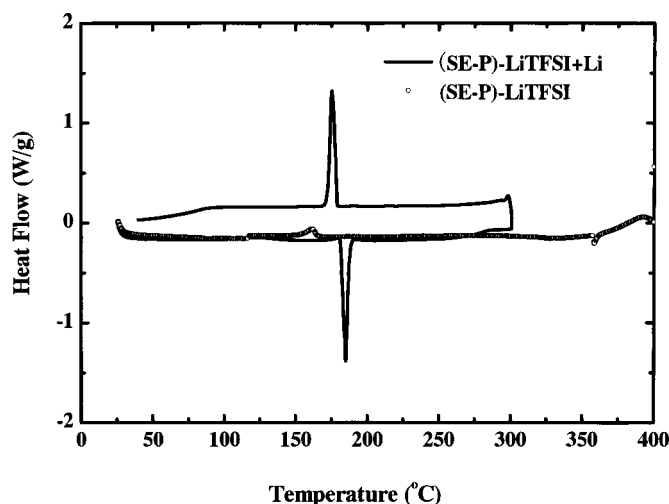
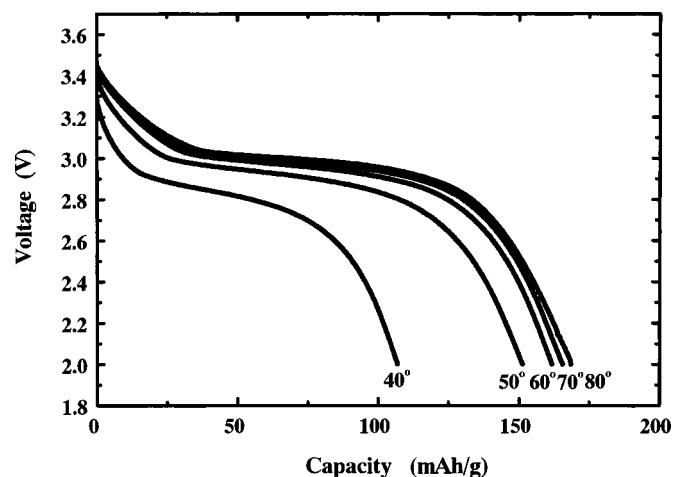
Table I. Fitted results of the experimental spectra after various cycles.

Cycle	$R_b(\Omega)$	$R_{(PE/Li)}(\Omega)$	$Q_{(PE/Li)}$	n
0	27.76	50.68	1.49×10^{-6}	0.8659
1	26.30	52.66	3.28×10^{-6}	0.7803
10	25.66	48.79	4.09×10^{-6}	0.7792
30	24.39	48.21	4.75×10^{-6}	0.7777
50	23.17	47.78	5.48×10^{-6}	0.7708
100	22.87	49.52	6.72×10^{-6}	0.7612
200	21.14	55.22	6.64×10^{-6}	0.7650

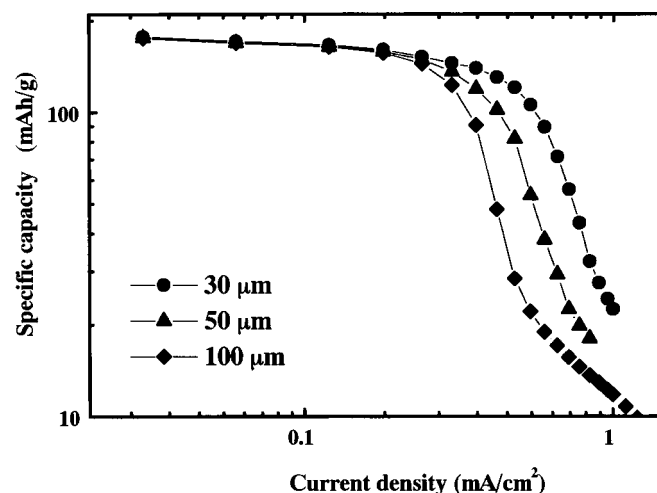
temperature over 60°C. The cell delivered a rechargeable capacity of 160 mAh/g with a very flat potential plateau at *ca.* 3.0 V vs. Li/Li⁺ at 60°C, corresponding to a specific energy of 450 Wh/kg of pure oxide.

For EV battery application, both the specific energy and rate capability are of primary importance. In a solid-state lithium/polymer battery, the polymer electrolyte film serves as a separator as well as an electrolyte medium providing an ion transportation path. Use of an ultrathin film is expected to increase its energy density. However, if the electrolyte film is too thin, it will cause an accidental short circuit, especially in the case of a large size battery. To improve reliability, the use of a polymer electrolyte with high mechanical resistance and dimensional stability is needed. As demonstrated above, the block-graft copolymer electrolyte has excellent mechanical properties which makes feasible film fabrication as thin as 10 μm. Figure 11 shows the plots of discharge capacity vs. discharge current of Li/Li_xMnO₂ cells at 80°C containing polymer electrolyte films of from 30 to 100 μm. The cell was discharged to 2.0 V at various discharge currents from 0.05 to 1.0 mA/cm². The charge current density was always set at 0.05 mA/cm². The difference in the discharge capacity among the three cells was detected at a current density over 0.25 mA/cm², corresponding to C/3. The cell using 30 μm thickness film showed better rate capability, delivering a capacity of 100 mAh/g even at a current density of 0.7 mA (1C). In the case of a liquid-electrolyte-based electrochemical cell, as the transportation of Li ion in the electrolyte is generally fast enough, to not be rate determining the discharge rate capacity is greatly influenced by both the diffusion rate of Li⁺ in the cathode crystal lattice and the particle size. For example, the limiting current, i_l , in the cell is governed by

$$i_l = 2nFCD/(1 \cdot t_+)r \quad [1]$$

**Figure 9.** The thermal stabilities of the SE-P polymer electrolyte alone and it in contact with metallic lithium.**Figure 10.** The discharge curves of a Li/SE-P/Li_xMnO₂ cell containing a 100 μm thick SE-P polymer electrolyte film at temperatures varying from 40 to 80°C.

where F is the Faraday constant, C is the concentration of the electrolyte, n is the number of equivalents of electrons transferred, D is the diffusion coefficient of Li⁺, t_+ is the transport number of Li⁺, and r is the radius of the active material. However, for a true solid-state polymer cell consisting of a metallic lithium, a polymer membrane, and a porous composite electrode, as Doyle and Newman proposed,¹⁹ at high current density, the low rate of the transport in the electrolyte phase is the main factor causing the voltage sharp drop in cell voltage. At low current density, the concentration of electrolyte is nearly constant, then the ohmic drop can be expected to dominate the current distribution in the porous electrode. The ohmic drop may be determined by both the electrode thickness and the interfacial resistance of the polymer electrolyte/active material. As demonstrated in our previous work,¹⁶ the interfacial resistance of the polymer electrolyte/active material is governed by the compatibility of a polymer electrolyte with the cathode material, and it is much more direct than the ionic conductivity of the polymer electrolyte in terms of the effect on rate capability. However, when the applied current is large up to a definite extent, the transport of Li⁺ in the polymer electrolyte (in the composite electrode or the electrolyte separator), which is directly linked to its ionic conductivity and the thickness of the electrolyte film, most likely becomes the rate-

**Figure 11.** The plots of discharge capacity vs. discharge current of Li/SE-P/Li_xMnO₂ cells at 80°C containing various thickness SE-P polymer electrolyte films, varying from 30 μm to 100 μm.

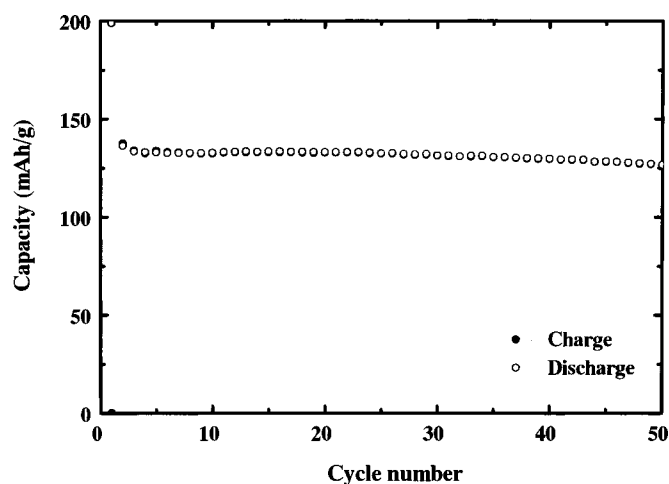


Figure 12. The cycle profile of a Li/SP-E/Li_xMnO₂ cell containing a 50 μm thick SE-P polymer electrolyte film at 80°C.

determining step that governs the cell discharge process. The thinner the electrolyte film is, the lower the electrode polarization will be.

The cycle life of an SE-P polymer electrolyte cell at 80°C is shown in Fig. 12. The charge/discharge efficiency of the cell is over 99.5%, showing a good cycle life and retention of 95% of the initial capacity after 50 cycles at 80°C.

Conclusion

The block-graft electrolyte copolymer consisted of a backbone molecule of polystyrene and a graft molecule of PEO with a MS. The electrolyte ionic conductivity is fair, $\sim 10^{-4}$ S cm⁻¹ at 60°C, being ten times more resistive than similar PEO electrolyte but showing ionic conductivity enhancement below 60°C. Having a special MS structure, the dimensional stability of this polymer film is outstanding. It is easy to make a feasible thin film without the risk of a short circuit due to the progressive creep of the polymer electrolyte film. High interfacial stability, thermal stability with a metallic lithium electrode, and electrochemical stability to 3.8 V vs. Li⁺/Li on a carbon-containing composite electrode make the block-graft copolymer a good candidate for extra-thin-film lithium-polymer batteries.

An all solid-state Li/Li_xMnO₂ battery containing a block-graft copolymer electrolyte delivers a rechargeable capacity of 160

mAh/g of Li_xMnO₂ with a very flat working voltage plateau at ca. 3.0 V vs. Li/Li⁺ at the C/3 rate at 60°C, corresponding to a specific energy of 450 W/kg of active material. The electrolyte film thickness critically affect its rate capability. The thinner films give better rate capabilities with a cell containing a 30 μm electrolyte delivering a capacity of 110 mAh/g at a rate of 1C. Preliminary results confirm the fair conductivity and high mechanical stability of the block-graft copolymer. There is high potential for the application of the electrolyte to extra-thin-film lithium/polymer batteries with high-energy density, good rate capability, and high safety.

Acknowledgments

The authors would like to thank the Japan Society for the Promotion of Science (JSPS) for partially funding the project.

The National Institute of Advanced Industrial Science and Technology assisted in meeting the publication costs of this article.

References

1. M. B. Armand, J. M. Chabagno, and M. J. Duclot, in *Fast Ion Transport in Solids*, P. Vashista, J. N. Mundy, and G. K. Shenoy, Editors, P. 131, North-Holland, Amsterdam (1979).
2. J. Przulski, K. Such, H. Wycisk, and W. Wieczorek, *Synth. Met.*, **35**, 241 (1990).
3. F. Croce, G. B. Appetechi, L. Persi, and B. Scrosati, *Nature (London)*, **394**, 456 (1998).
4. H. Y. Sum, H. J. Sohn, O. Yamamoto, Y. Takeda, and N. Imanishi, *J. Electrochem. Soc.*, **146**, 1672 (1999).
5. M. Watanabe and A. Nishimoto, *Solid State Ionics*, **79**, 306 (1995).
6. S. Sylla, J. Y. Sanchez, and M. Armand, *Electrochim. Acta*, **37**, 1699 (1992).
7. G. Negasuramanian, E. Peled, A. I. Attia, and G. Halpert, *Solid State Ionics*, **67**, 51 (1993).
8. Y. Dai, Y. Wang, S. G. Greenbaum, S. A. Bajue, D. Golodnitsky, G. Ardel, E. Strauss, and E. Peled, *Electrochim. Acta*, **10-11**, 1557 (1998).
9. E. Peled, D. Golodnitsky, G. Ardel, J. Lang, and Y. Lavi, *J. Power Sources*, **54**, 496 (1995).
10. K. Se, K. Miyawaki, K. Hirahara, A. Takano, and T. Fujimoto, *J. Polym. Sci., Part A: Polym. Chem.*, **36**, 3021 (1998).
11. M. Yoshio, H. Nakamura, and Y. Xia, *Electrochim. Acta*, **45**, 273 (1999).
12. Y. Xia, T. Fujieda, K. Tatsumi, P. P. Prosini, and T. Sakai, *J. Electrochem. Soc.*, **147**, 2050 (2000).
13. K. Se, K. Adachi, and T. Kotaka, *Polym. J. (Tokyo, Jpn.)*, **13**, 1009 (1981).
14. K. Se, K. Adachi, and T. Kotaka, *Rep. Prog. Polym. Phys. Jpn.*, **22**, 393 (1979).
15. K. Se, K. Adachi, and T. Kotaka, *Rep. Prog. Polym. Phys. Jpn.*, **22**, 397 (1979).
16. C. Wang, Y. Xia, T. Fujieda, T. Sakai, and T. Muranaga, *J. Power Sources*, **103**, 223 (2002).
17. G. B. Appetecchi, S. Scaccia, and S. Passerini, *J. Electrochem. Soc.*, **147**, 4448 (2000).
18. Y. Xia, T. Sakai, C. Wang, T. Fujieda, K. Tatsumi, K. Takahashi, A. Mori, and M. Yoshio, *J. Electrochem. Soc.*, **148**, A112 (2001).
19. M. Doyle and J. Newman, *J. Electrochem. Soc.*, **140**, 1526 (1993).